Korean J. Chem. Eng., 33(8), 2374-2383 (2016)
DOI: 10.1007/s11814-016-0078-6

pISSN: 0256-1115
eISSN: 1975-7220

Kinetic, thermodynamic and equilibrium studies on removal of hexavalent chromium from aqueous solutions using agro-waste biomaterials, casuarina equisetifolia L. and sorghum bicolor

Mokkapati Ramya Prasanthi*, Mokkapati Jayasravanthi, and Ratnakaram Venkata Nadh***,†**

*Department of Chemistry, ANUCET, Acharya Nagarjuna University, Guntur - 522510, India
**Department of Biotechnology, Acharya Nagarjuna University, Guntur - 522510, India
***GITAM University - Bengaluru Campus, Karnataka - 561 203, India
(*Received 30 August 2015 • accepted 15 March 2016*)

Abstract−Removal of Cr(VI) by biosorption on two agro waste materials, casuarinas fruit powder (CFP) and sorghum stem powder (SSP), has been investigated. The prepared adsorbent materials were characterized by SEM, EDX, FTIR and BET. These biomaterials effectively removed Cr(VI) with a maximum removal of 93.35% and 63.75% using 15 gL^{-1} and 5 gL^{-1} of CFP and SSP, respectively, at 60 °C with 20 mgL^{-1} initial Cr(VI) concentration in solution. In both cases of adsorbents, kinetic data of adsorption fitted well in pseudo-second-order in terms of correlation coefficient (R^2). This helps in proposing the process of adsorption as chemical coordination, which is correlated with the thermodynamic study results conducted at different values of temperature. Langmuir, Freundlich and D-R models were evaluated for description of metal sorption isotherms. Values of coefficients of intra-particle diffusion and mass transfer have also been determined at different values of temperature.

Keywords: Casuarinas Fruit Powder, Sorghum Stem Powder, Removal, Chromium, Adsorption

INTRODUCTION

Chromium is a type of heavy metal involved in a number of industrial applications like textile dyeing, pigment, leather tanning, electroplating, oil refineries, fertilizers, production of ferrochrome, steel and cement, fungicides, and metal finishing, causing water pollution, which is a major environmental concern [1]. Chromium exists in two stable oxidation states: relatively innocuous and immobile Cr(III) and a readily movable and strong oxidizing agent Cr(VI). This common aquatic pollutant in its hexavalent state Cr(VI) released by industrial activities into natural waters has detrimental effects on both the living organisms and the ecosystems [2,3]. The permissible limit of Cr(VI) into the water bodies given by WHO is 0.05-1 mgL^{-1}; however, a report by WHO, 2004 says that a much higher concentration around 100 mgL^{-1} of Cr(VI) would be present in the untreated effluent of an electroplating industry [4]. Therefore, to bring down the concentration of Cr(VI) to acceptable levels, almost all the industries must treat their effluents before disposal.

Hexavalent chromium is capable of being absorbed through the skin, which makes it highly toxic to living organisms [5]. It has very adverse effects if exposed strongly causing skin irritation to lung cancer, kidney, liver and gastric damage, epigastric pain, nausea, vomiting, severe diarrhea and hemorrhage; and due to its mutagenicity and carcinogenicity to human beings, it belongs to group "A" human carcinogen [6,7].

†To whom correspondence should be addressed.
E-mail: doctornadh@yahoo.co.in

The downside of many conventional techniques for the removal of Cr(VI) from aqueous solutions such as chemical reduction, precipitation, ion-exchange, and adsorption (using commercial charcoal) is that they are expensive for large-scale treatment of industrial effluents, which is making these procedures unaffordable for developing nations [8]. Emphasizing on this aspect, many researchers have used unconventional materials as adsorbents for the removal of Cr(VI) from aqueous solutions and industrial effluents [9-23].

To potentially remove the toxic heavy metals from water streams, biosorption is an attractive alternate to traditional industrial effluent treatment processes as it utilizes the biological materials as adsorbents which have high surface area and electric charges to accumulate heavy metals [24-32]. Polar functional moieties (containing heteroatoms) adsorb Cr(III) because these heteroatoms donate their lone pairs of electrons to Cr(VI), and in the process reduced Cr(VI) to Cr(III) [33]. The brown macroalga Pelvetia canaliculata was used as a natural electron donor for the reduction of Cr(VI) to Cr(III) at acidic pH followed by removal of other metal ions present in the mixture by ion-exchange [34]. In addition, removal of Cr(III) by different biosorbents was studied recently [35-39]. It has been reported in the literature that, in comparison to the crude ones, the chemically modified natural adsorbents are much more advantageous in their pollutant removal efficiency from aqueous environment [8].

Moreover, due to the capability of lowering heavy metal concentration to mgL^{-1} level, wide range of availability and ecofriendly nature, the usage of biopolymers from agricultural wastes as adsorbents is attracting many industries [40]. Hence, in the present work, the chemically modified powders of two abundantly available agricultural wastes (casuarinas fruit and sorghum stem) have been used

for the removal of Cr(VI) from aqueous solutions. Additionally, the kinetics and equilibrium of adsorption process have also been evaluated to classify the mechanism of adsorption process as intrinsic adsorption, which is based on the surface area of adsorbent or the coulombic interaction, which is based on the electrostatic interaction between opposite charges on adsorbents and solute [2,41].

EXPERIMENTAL

Raw materials such as casuarinas fruit and sorghum stem for the preparation of adsorbents are available abundantly in nature. The left-over material of the dehisced cones of casuarinas trees and the left over sorghum stems after harvesting of the grains were collected from the coastal Andhra Pradesh, India. They were cleaned with distilled water and then washed with formaldehyde solution (2%), which helps to reduce organic leaching and prevent mold growth during batch sorption [42] and completely air dried. The dried materials were pulverized into fine powder and sieved with standard sieves of particle size 0.3-1.0 mm. Then the finest powders of casuarinas fruit (CFP) and sorghum stem (SSP) were treated with 1 N H_2SO_4 and allowed to soak for 24 h at room temperature. The samples were oven dried and allowed to cool to room temperature, and thereafter used for adsorption studies without further modification. The preliminary studies show that the removal capacity of these treated adsorbents is higher by about 30% compared to those of untreated adsorbents. Hence, treated samples were used throughout the study. The biosorbent was stored in clean air tight containers. All the chemicals used were of analytical grade.

1. Instrumentation

The physico-chemical characterization of adsorbents was performed by scanning electron microscopy (SEM) coupled to energy-dispersive X ray spectroscopy (EDX) (F E I Quanta FEG 200 - High resolution scanning electron microscope), which allows the identification and quantification of the metal ions on the surfaces of the adsorbents. The Fourier transform infra red (FT-IR) spectra of the crude and metal treated adsorbents were performed using Bruker, ALPHA-T to identify the active functional groups responsible for the adsorption. Specific surface areas and pore sizes of the adsorbents were determined with Brunauer Emmett Teller (BET) N_2 surface area analyzer (Nova 1000 Ver. 3.70).

2. Preparation of Synthetic Solutions

The standard Cr(VI) stock solution was prepared by dissolving potassium dichromate in deionized water and diluted according to the required concentrations. The initial Cr(VI) concentration of the untreated sample was 20 mgL^{-1}. The typical pH of the experiments was about 1, and it was adjusted to the desired value by the addition of few drops of 0.1 M HCl or 0.1 M NaOH.

3. Batch Adsorption Studies

The experiments were performed in batch process by taking 50 mL of metal ion solution in 250 mL conical flask and using CFP and SSP as adsorbents. While observing the effect of each parameter, the values of remaining parameters were kept constant. For each adsorbent, the metal ion removal efficiency was determined in individual experiments. The range of experimental conditions of different parameters were 1 to 20 gL^{-1} (adsorbent dose), 0.5 to 180 min (time), 1 to 5 (pH), 30 to 70 °C (solution temperature), and 50 to 300 rpm (speed of rotation). In each experiment, the metal ion solution was equilibrated with adsorbent and then aliquots were withdrawn. After centrifugation, the final Cr(VI) concentrations were measured by diphenyl carbazide method [43]. Each experiment was repeated thrice and average of the results was reported. The adsorption capacity and the percent removal of metal ions were determined by the following equations.

$$\text{Percent removal of Cr(VI)} = \frac{C_e - C_o}{C_e} \times 100 \quad (1)$$

$$q_e = \frac{C_o - C_e}{w} \times V \quad (2)$$

$$q_t = \frac{C_o - C_t}{w} \times V \quad (3)$$

where C_o is the initial concentration of Cr(VI) in solution, C_e is the final concentration of Cr(VI) in solution after adsorption, C_t is the concentration of Cr(VI) in solution after adsorption at any time

Table 1. Linear and nonlinear forms of adsorption kinetics and isotherm models

Model	Non-linear form	Linear form	Reference
Adsorption kinetics models			
Pseudo-first-order	$\frac{dq_t}{dt} = k_1(q_e - q_t)$	$\ln(q_e - q_t) = \ln q_e - k_1 t$	[25]
Pseudo-second-order	$\frac{dq_t}{dt} = k_2(q_e - q_t)^2$	$\frac{t}{q_t} = \frac{1}{k_2 q_e^2} + \frac{t}{q_e}$	[26]
Elovich	$\frac{dq_t}{dt} = \alpha \exp^{-\beta q_t}$	$q_t = \frac{1}{\beta}\ln\alpha\beta + \frac{1}{\beta}\ln t$	[13]
Intra-particle diffusion	-	$q_t = K_d t^{1/2} + \theta$	[13,20]
Adsorption isotherm models			
Langmuir	$q_e = \frac{q_m K_L C_e}{1 + K_L C_e}$	$\frac{C_e}{q_e} = \frac{C_e}{q_m} + \frac{1}{K_L q_m}$	[16,22]
Freundlich	$q_e = K_F C_e^{1/n}$	$\log q_e = \log K_F + \frac{1}{n}\log C_e$	[16,22]
Dubinin-Radushkevich	$q_e = q_D \exp^{-B_D \varepsilon^2}$	$\ln q_e = \ln q_D - B_D \varepsilon^2$	[22]

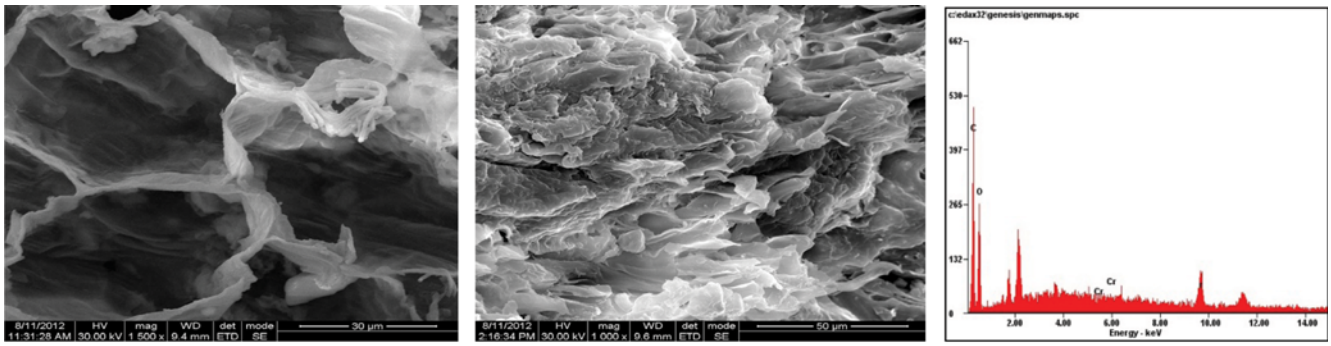

Fig. 1. Scanning electron micrographs of CFP (a) before adsorption, (b) after adsorption and (c) EDX energy profile of CFP after adsorption.

t, q_e (mgg^{-1}) is the adsorption capacity of the adsorbent at equilibrium, q_t (mgg^{-1}) is the adsorption capacity of the adsorbent at time t, V(L) is the volume of suspension, and W(g) is the mass of adsorbent.

4. Adsorption Kinetics

Kinetics of adsorption was carried out by employing pseudo-first-order [44] and pseudo-second-order [45] kinetic equations to examine the mechanism of Cr(VI) adsorption on to these adsorbents. Adsorption kinetics and isotherms models studied in the present study are shown in Table 1.

In the Table 1 q_t and q_e (mgg^{-1}) are the amounts of chromium adsorbed on adsorbent material at time t and at equilibrium, respectively; k_1 and k_2 are the corresponding pseudo-first and second-order adsorption rate constants; α is the initial Cr(VI) sorption rate (mgg^{-1} min^{-1}); β is the desorption constant (gmg^{-1}) during any one experiment; K_d is the rate constant of the intraparticle transport ($mgg^{-1}min^{1/2}$); θ is the constant related to the thickness of the boundary layer (mgg^{-1}); C_e is the equilibrium concentration (mgL^{-1}); q_e is the monolayer adsorption capacity (mgg^{-1}); K_L (Lmg^{-1}) is the Langmuir constant related to the energy of sorption; K_F and n are Freundlich constants for a given adsorbate and adsorbent at a particular temperature; B_D is a constant related to the mean free energy of adsorption per mole of the adsorbate (mol^2kJ^{-2}); q_D (DR isotherm constant) is the theoretical saturation capacity (mgg^{-1}); and ε is the Polanyi potential, which is equal to RT ln(1+(1/C_e)), where R ($Jmol^{-1}$ K^{-1}) is the gas constant; and T (K) is the absolute temperature.

5. Adsorption Thermodynamics

Thermodynamic parameters such as change in free energy (ΔG), enthalpy (ΔH) and entropy (ΔS) were determined using the below equations. The apparent equilibrium constant (K_C) of the biosorption is defined as $K_C=C_{ad,eq}/C_{eq}$, where $C_{ad,eq}$ and C_{eq} are the concentration of Cr(VI) on the adsorbent and residual Cr(VI) concentration at equilibrium, respectively. Thermodynamic equilibrium constant (K_C) of the adsorption system is related to free energy change as following equation [46].

$$\Delta G^{o}=-RT\ln K_c \quad (4)$$

where ΔG is free energy change, R is the universal gas constant, 8.314 $Jmol^{-1}K^{-1}$ and K is the absolute temperature [27]. Thermodynamic parameters were calculated using van't Hoff equation as given below.

$$\ln K_c=-\frac{\Delta G}{RT}=-\frac{\Delta H}{RT}+\frac{\Delta S}{R} \quad (5)$$

The plot of ln K_C as a function of 1/T yields a straight line. ΔH and ΔS can be calculated from the slope and intercept, respectively.

RESULTS AND DISCUSSION

1. SEM, EDX, FT-IR and BET Studies

Scanning electron microscopy dictates the nature of adsorption process through visible observation of the surface texture and porosity of the samples and is given in Fig. 1. Before adsorption, rough surface with some pores was visible on the surface of each adsorbent (Fig. 1(a)), whereas, a smooth surface covering of the pores can be observed after adsorption (Fig. 1(b)). EDX studies were carried out to determine the chemical composition of adsorbents, CFP (wt% of elements) before adsorption: C-46.84, O-40.49, Fe-0.45, Cr-0.00; SSP:C-61.26, O-34.69, Fe-0.22, Zn-0.26, Cr-0.00; after adsorption: C-58.53, O-38.44, Fe-01.34, Cr-0.15; SSP: C-53.47, O-41.46, Fe-0.34, Zn-0.31, Cr-0.16 (Fig. 1(c)). In both absorbents, presence of stretching for C-O, C=O and aliphatic C-H can be confirmed from peaks in the range of 1,023-1,039 cm^{-1}, 1,614-1,689 cm^{-1} and 2,917-2,920 cm^{-1} respectively. Presence of amine/amide group is evident from the peaks in the ranges of 3,400-3,250 cm^{-1} (N-H str) and 1,650-1,580 cm^{-1} (N-H bend). But, additional peaks in CFP above 3,000 cm^{-1} indicate the =C-H stretching and further C=C stretching can be observed from peaks in the range of 1,450-1,550 cm^{-1}. Broad peaks in the range of 3,305-3,320 cm^{-1} indicate the presence of carboxylic acid groups in SSP, whereas, dominant sharp peak at 3,737 cm^{-1} indicates phenolic groups in CFP (Fig. 2).

EDX and FT-IR observations correlate with the compositions of SSP - cellulose, hemicelluloses, lignin, cutin, silica [47], and CFP - α-pinene, benzaldehyde, 1,8 cineole, furanoid, α-campholenal, 4-terpineol, α-terpineol, α-terpinyl acetate, spathulenol, caryophyllene-oxide, guaiol [48]. The presence of functional groups like acid, alcohol and amine is evident from these studies. Protons of phenols/alcohols and carboxylic acid groups in these biosorbent facilitate them for ions getting exchanged during the adsorption process (Fig. 3). Hydroxyl groups in these biopolymers may function as donors. Hence the de-protonation of hydroxyl groups can be involved in the co-ordination with metal ions [49]. Moreover, pres-

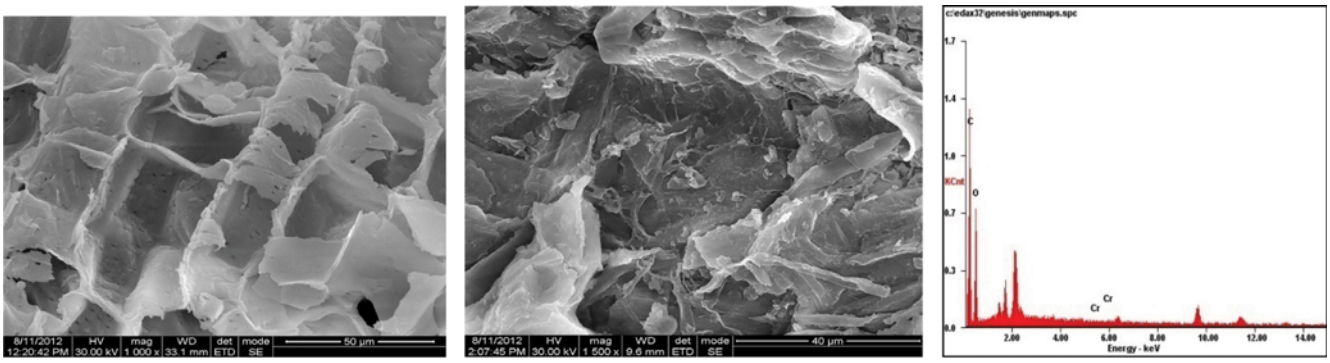

Fig. 2. Scanning electron micrographs of SSP (a) before adsorption, (b) after adsorption and (c) EDX energy profile of SSP after adsorption.

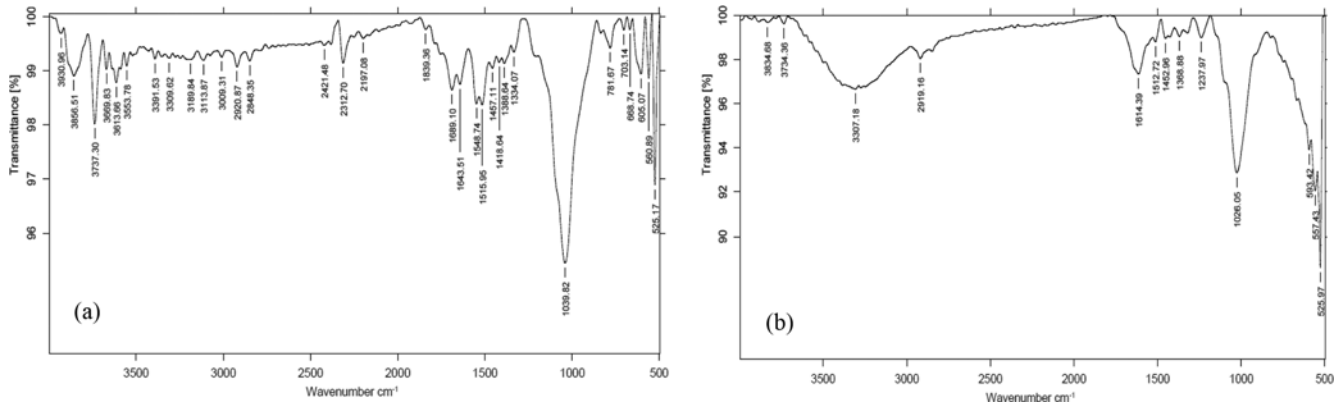

Fig. 3. Fourier Transform Infra Red spectrum of acid treated (a) CFP and (b) SSP.

ence of more number of peaks in CFP compared to SSP can be explained based on presence of good number of phytochemicals as mentioned above.

Acid treatment improved the specific surface area and total pore volume of crude SSP from 5.0030 m^2g^{-1} to 24.7714 m^2g^{-1} and 0.00235 $cm^3\ g^{-1}$ to 0.02090 $cm^3\ g^{-1}$, respectively. Similarly, specific surface area and total pore volume of crude CFP increased from 1.2270 m^2g^{-1} to 41.8931 m^2g^{-1} and 0.00277 $cm^3\ g^{-1}$ to 0.03119 $cm^3\ g^{-1}$ by acid treatment.

2. Studies on Effect of Contact Time and Adsorption Kinetics

To better understand the Cr(VI) sorption characteristics by the two adsorbents, SSP and CFP, both kinetic and equilibrium models were used to describe the data. Changes in Cr(VI) concentrations over time were investigated by varying the contact time from 0.5 to 180 min, while other parameters were kept constant and are shown in Fig. 4. As the contact period between adsorbent and Cr(VI) ions increases the adsorption of metal ion increases as more time familiarizes the metal ion to make an attraction complex with the adsorbent [50]. The results revealed that the saturation level of adsorption was reached at equilibration point of 120 min in case of SSP and 150 min in case of CFP as adsorbents and remained constant. This is apparent from the fact that a large number of sites are available for sorption during the initial stage, and few minutes later the remaining vacant surface sites are hard to be occupied due to repulsive forces between the Cr(VI) on the solid

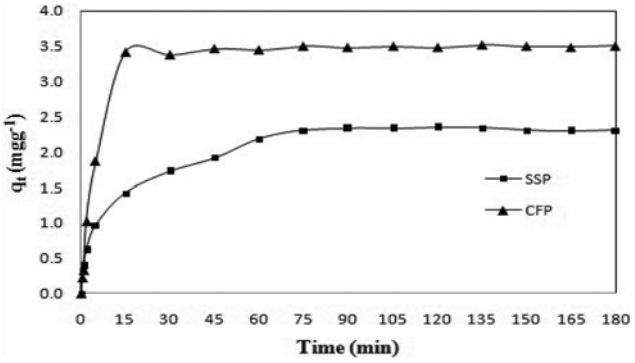

Fig. 4. Effect of contact time on Cr(VI) sorption, at 30 °C, 20 mgL^{-1} Cr(VI) and 200 rpm.

and the aqueous phases [51,52]. The better performance of SSP and CFP compared to the earlier used adsorbents is manifested from the optimum period of 120 and 150 min, respectively, in the present case because it is 180 min using Bengal gram (*Cicer arientinum*) [16] and Erythrina Variegata Orientalis leaf powder (Gannavarapu Venkata Vamsi Aditya et al., 2012), 80 min using *Fagas orientalis* L. saw dust [53], 70 min using a low cost fertilizer industry waste material [18], 120 min using biomass of filamentous algae spirogyra species [17].

Pseudo-first-order [44] and pseudo-second-order [45] kinetic

Table 2. Adsorption kinetic parameters for the removal of Cr(VI) using CFP and SSP

Adsorbent	Pseudo-first-order			Experimental value	Pseudo-second-order		
	q_t (mg g^{-1})	k_1 (min^{-1})	R^2	q_t (mg g^{-1})	q_t (mg g^{-1})	k_2 (g mg^{-1} min^{-1})	R^2
SSP	1.190	0.018	0.779	2.400	2.433	0.059	0.997
CFP	0.950	0.016	0.600	3.600	3.623	0.062	0.998
Adsorbent	Elovich model			Weber's intra-particle diffusion model			
	α ($mgg^{-1}min^{-1}$)	β (gmg^{-1})	R^2	K_d ($mgg^{-1}min^{1/2}$)		θ (mgg^{-1})	R^2
SSP	1.202	2.564	0.979	0.159		0.575	0.866
CFP	2.319	1.684	0.899	0.221		1.177	0.659

equations were employed to examine the mechanism of Cr(VI) adsorption on to these adsorbents, as the literature survey clearly shows that the sorption of Cr(VI) from aqueous solution is either first- or second-order (Table 1). For example, removal of Cr(VI) by *Tamarindus Indica* seed (TS), crushed coconut shell (CS), almond shell (AS), ground nut shell (GS) and walnut shell (WS) follows the pseudo-first-order biosorption [54], whereas, pseudo-second-order was found to correlate with the experimental data well by using peat, leaf mold and granular activated carbon [55-57], cornelian cherry, apricot stone and almond shell [13], fertilizer industry waste material [18], as adsorbents. In the present case, kinetic data is in good agreement with pseudo-second-order in terms of coefficient of determination (R^2) than pseudo-first-order and the adsorption kinetic parameters are given in Table 2.

In addition, the simple Elovich equation was also employed for its applicability on the adsorption process [13]. The interactions between adsorbate and adsorbent materials follow film diffusion, pore diffusion and intra-particle transport, among which pore diffusion and intra-particle diffusion are often rate-limiting in a batch reactor, whereas film diffusion is more likely the rate-limiting step for a continuous flow system [13]. Hence, Weber's intraparticle diffusion model was analyzed. Biosorption is a complex process, mainly comprised of ion exchange, chelation and adsorption by physical forces and entrapment in inter and intra-fibrillar capillaries and space of the structural polysaccharide network as a result of the concentration gradient and diffusion [58]. In addition, non-conventional adsorbents contain cellulose, and the polar hydroxyl groups on the cellulose could be involved in chemical reaction and hence bind heavy metals from solutions [59]. Thus, in the present case also, the mechanism of adsorbate and adsorbent interaction as chemical coordination is explained by two stages of the adsorption of Cr(VI), i.e., the first stage, solute uptake, which is the immediate solute uptake achieved within less time, followed by the second stage, which is the subsequent uptake of solute, which continues for a long time period [13]. Similar observations were reported on removal of Cr(VI) using fertilized industry waste material [18]. Both the Elovich and Weber intraparticle diffusion models showed reasonably good correlation (Table 2).

3. Effect of Adsorbent Dose

The varying pattern of adsorption with adsorbent dose gives the adsorption efficiency of adsorbent. By observing the results, it was clear that the adsorbent dose can greatly affect the adsorption of Cr(VI), and it was increased with increase in adsorbent concentration in reaction mixture due to the availability of more active sites on the adsorbent surface [60,61]. But unit adsorption was decreased with the increase in adsorbent dosage which may be due to overlapping of adsorption sites as a result of overcrowding of adsorbent particles, shown in (Fig. 5 and 6). Higher Cr(VI) sorption at lower levels of adsorbents, CFP and SSP could be due to the higher metal to biosorbent ratio, which decreases as the biomass quantity is increased [62].

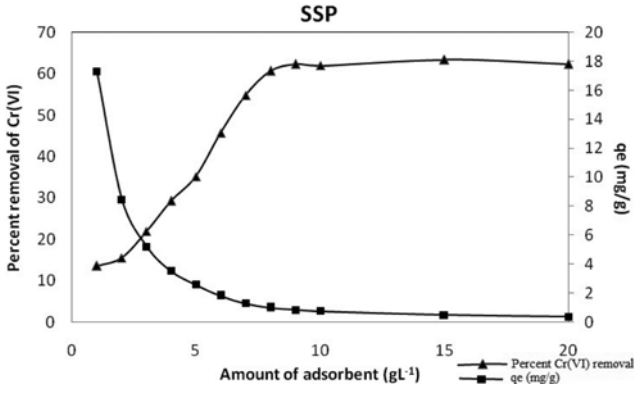

Fig. 5. Effect of adsorbent dose on Cr(VI) sorption by SSP, at 30 °C, pH 1, 20 mgL^{-1} Cr(VI) and 200 rpm.

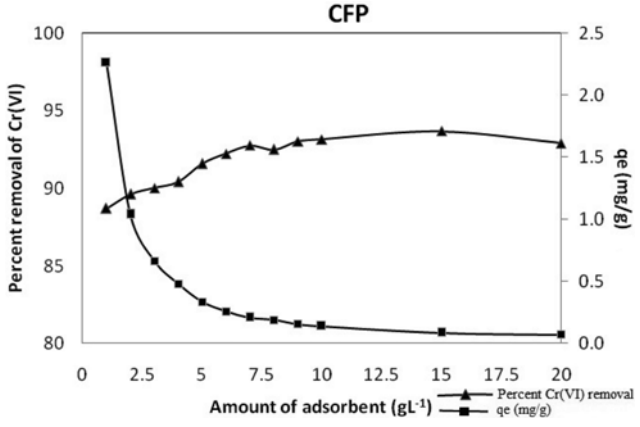

Fig. 6. Effect of adsorbent dose on Cr(VI) sorption by CFP, at 30 °C, pH 1, 20 mgL^{-1} Cr(VI) and 200 rpm.

4. Effect of pH

In addition to surface charge of the adsorbent, the other parameters influencing the adsorption are degree of ionization and the type of adsorbate species, which in turn depends on pH of the solution. Moreover, the stability of the chromium in its two predominant oxidation states (+6 and +3) is also dependent on the pH of the system [63,64]. Hence, it was thought important to study the effect of pH on the removal of Cr(VI). It is reported in the literature that Cr(VI) is predominantly removed in the pH vicinity of 1 [13]. However, maximum Cr(VI) removal was observed at pH 2.0 using a low cost fertilizer industry waste material [18], waste pomace of olive oil factory [46], husk of Bengal gram (*Cicer arientinum*) [16]. However, higher removal of Cr(VI) was observed using chitosan as an adsorbent at pH 5 [65].

Chromium (VI) exists as neutral $Cr(OH)_3$ species at pH between 7 and 12. At pH 7, the chromium presents as neutral $Cr(OH)_3$ species, which has low affinity for electrostatic interaction with the functional groups present on adsorbent [17]. The removal of metal ion at pH values higher than 12 could be attributed to the formation of their hydroxides, which results in precipitates [66]. Moreover, the literature survey shows that with increase in the pH, from 4.0 to 11.0, the degree of protonation of the surface reduced gradually and hence decreased adsorption was noticed [10,67]. Hence the adsorption experiments were better performed in acidic pH (1 to 5) to avoid precipitate formation and for focus study.

Adsorption efficiency of metal ion with varying acidic pH is depicted in Fig. 7. The removal of Cr(VI) is greatly affected by changes in pH with the use of CFP and SSP as adsorbents because the functional groups responsible for binding of metal ions in the adsorbent are affected [59]. At lower pH levels, the adsorption of the chromium ions reaches a maximum of 82 and 92% at pH for SSP and CFP, respectively. The effect of pH can be better explained by considering the surface charge on the adsorbent materials. In general, the ionic attraction attained by the functional groups (carboxylate and -OH groups) present on biosorbent leads to the adsorption of cations on it. However, in the present case, anionic forms of chromium(VI) are adsorbed by protonated amines/amides of biomass, as these groups act as anion-adsorption sites. The role of protonated functional groups in removal of anionic forms of chromium(VI) in acidic pH was well documented by An and Dultz [68].

Chromium exhibits different types of Ph-dependent equilibria in aqueous solutions. As the pH is shifted, the equilibrium will also shift; in the pH range 2-6, $HCrO_4^-$, and $Cr_2O_7^{2-}$, ions are in equilibrium. At lower pH (pH<2.0) values, $Cr_3O_{10}^-$ and $Cr_4O_{13}^{2-}$ species are formed. As the optimum pH for biosorption of hexavalent chromium on CFP and SSP was observed at pH 1.0, the chromium was removed in its polymerized form because it is well known that the dominant form of Cr(VI) at pH 1 is $HCrO_4^-$ [55], as comparable with the chromium removal by Bengal gram [16].

In the present case, an increase in the removal of Cr(VI) with a decrease of pH of the medium from 5 to 1 can be explained based on the existence of Cr(VI) in different forms of negatively charged chromium species (oxy anions like $HCrO_4^-$, $Cr_2O_7^{2-}$, CrO_4^{2-} etc.) in acidic medium. When pH is below 5, the presence of a large number of H^+ ions causes an increased protonation of adsorbent, which causes a strong electrostatic attraction between the oxyanions of Cr(VI) and positively charged surface of the adsorbent [69]. In some cases, Cr(VI) was completely reduced to Cr(III) by contact with biomass [70,71], but in the present case, the chromium remains in its +6 state, which is evident from the non-formation of characteristic green color of Cr(III).

5. Effect of Temperature of the Medium During Adsorption

Temperature of the medium has a critical impact on any reaction process to occur. During adsorption, the effect of temperature on the removal of Cr(VI) from aqueous solutions has significance to say whether the process is endothermic or exothermic and relates to the physisorption or chemisorptions. The removal of Cr(VI) using CFP and SSP as adsorbents with varying temperatures is shown in Fig. 8. The maximum adsorption of Cr(VI) was 92% at 50 °C using CFP and 63% at 60 °C using SSP. The adsorption percentage increased with an increase in temperature in case of SSP, whereas, in case of CFP, the adsorption percentage did not significantly change with increasing temperature.

In general, preferable binding can be expected at higher temperatures for endothermic reactions. Hence, in the present study, it indicates that the enthalpy change ΔH is positive (endothermic) due to increase in adsorption on successive increase in temperature. Further, negative ΔG values show that thermodynamically feasible and spontaneous nature of the adsorption process and positive value of ΔS reveals the increased randomness at the solid-solution interface during the adsorption of the Cr(VI) on the adsorbent

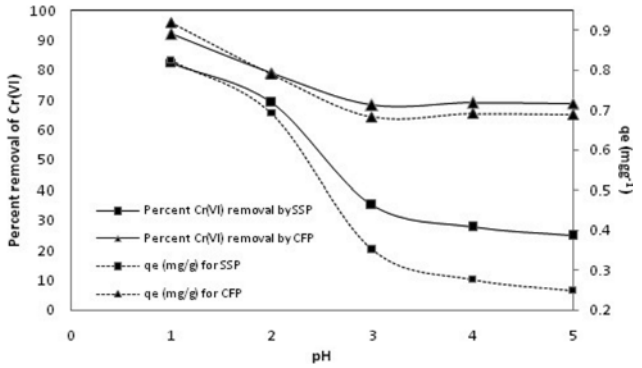

Fig. 7. Effect of pH on Cr(VI) sorption, at 30 °C, 20 mgL^{-1} Cr(VI) and 200 rpm.

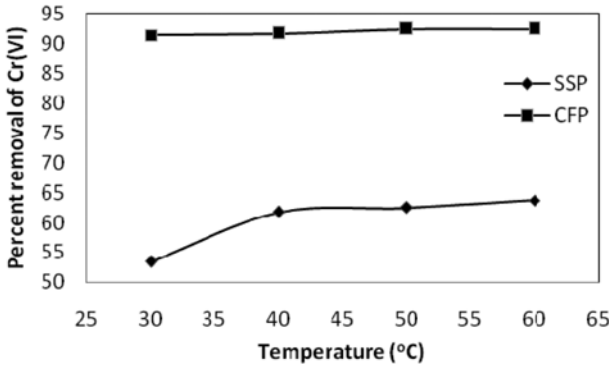

Fig. 8. Effect of temperature on Cr(VI) sorption by 5 gL^{-1} CFP at pH 3, 20 mgL^{-1} Cr(VI) and 200 rpm.

Table 3. Thermodynamic parameters at different temperatures for sorption of Cr(VI) on CFP and SSP

T (K)	SSP			CFP		
	ΔG ($Jmol^{-1}$)	ΔH ($Jmol^{-1}$)	ΔS ($JK^{-1}mol^{-1}$)	ΔG ($Jmol^{-1}$)	ΔH ($Jmol^{-1}$)	ΔS ($JK^{-1}mol^{-1}$)
303	−342.4	11182.3	38.7	−5942.3	4472.9	34.4
313	−1250.3			−6240.0		
323	−1371.8			−6717.4		
333	−1562.9			−6925.4		

material active sites. A similar observation of maximum adsorption of Cr(VI) by waste pomace was found at 333 K, which was endothermic but spontaneous under studied conditions [46]. Also, the rise in sorption capacity with temperature is because of rise in the kinetic energy of sorbent particles, which is due to increased collision frequency between sorbent and sorbate with increase in temperature and results in enhanced sorption on to the surface of the sorbent. Additionally, at high temperature, there may be an increase in number of active sorption sites due to bond rupture of functional groups on adsorbent surface, leading to enhanced sorption with the rise in temperature [72]. However, in case of CFP as adsorbent, the modest increase in Cr(VI) removal with change in temperature can be explained by the competitive dissolution of functional groups like tannins and other phenol/alcohol compounds in sorbing solution at high temperatures [73]. Thermodynamic parameters (ΔG, ΔH and ΔS) were calculated [46] and were given in Table 3.

6. Effect of Agitation

In earlier studies, removal of Cr(VI) increased with an increase in agitation speed and reached an optimum value like 120 rpm using the husk of Bengal gram (*Cicer arientinum*) [16] and *Rhizopus nigricans* [74], whereas, in the case of *Rhizopus arrhizus* [75] it was 100 rpm. Those observations were justified based on the fact that agitation facilitates proper contact between the metal ions in solution and the biomass binding sites and thereby promotes effective transfer of sorbate ions to the sorbent sites. In the present study also the effect of agitation was of same pattern that is the removal of Cr(VI) was increased with stirring rate and reached equilibrium at 250 rpm using CFP and SSP as adsorbents when studied in the range of 50 to 300 rpm. The effect of speed of rotation on adsorption capacity of SSP and CFP towards removal of Cr(VI) is shown in Fig. 9.

7. Effect of Initial Concentration of Metal Ion

The driving force to overcome all the mass transfer resistances of the metal between aqueous and solid phase is the initial metal concentration of the solution [76]. Incompletion of adsorption sites during adsorption reaction and the aggregation of adsorbent particles at higher concentration are the important factors which contribute to the adsorbate concentration effect. Fig. 10 shows the effect of metal ion concentration on its removal from the aqueous solution for adsorbent materials, CFP and SSP. A continuous decline of percentage removal with increase in metal ion concentration was observed. This appears to be due to the increase in the number of ions competing for the available binding sites in the biomass and also due to the lack of binding sites for the complexation of Cr ions at higher concentration levels.

8. Adsorption Isotherms

Adsorption isotherms are significant in describing the mechanism of adsorption for analyzing the interaction of metal ion on the surface of adsorbent. Langmuir and Freundlich adsorption isotherm equation were employed to evaluate the adsorption efficiency of each adsorbent. The values of characteristic parameters q_m and K_L are calculated from the slope and intercept of linear dependencies and the correlation coefficient R^2 associated to each model are given in Table 4.

Linear plots obtained for both Langmuir and Freundlich adsorption isotherms indicate best fitness of experimental data to corresponding models. The observed increase in uptake capacity of CFP and SSP with the increase of Cr(VI) ion concentration is due to higher availability of Cr(VI) ions in the solution, for the adsorption. Moreover, higher initial Cr(VI) concentration increased driving force to overcome all mass transfer resistance of metal ions

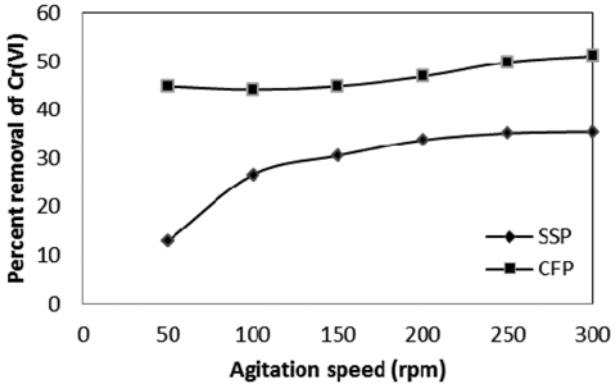

Fig. 9. Effect of agitation on Cr(VI) sorption by 5 gL^{-1} CFP/SSP at pH 1, 20 mgL^{-1} Cr(VI) and 200 rpm.

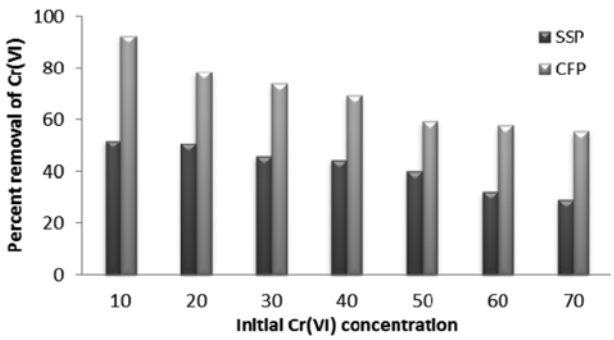

Fig. 10. Effect of initial Cr(VI) concentration on biosorption using 5 gL^{-1} CFP/SSP at pH 1, 30 °C and 200 rpm.

Table 4. Adsorption isotherm model parameters for the sorption of Cr(VI) on CFP and SSP

Langmuir isotherm			Freundlich isotherm			D-R isotherm		
Parameter	SSP	CFP	Parameter	SSP	CFP	Parameter	SSP	CFP
K_L (Lmg^{-1})	0.055	0.097	n	1.704	1.845	q_D (mol g^{-1})	3.669	6.110
q_m (mgg^{-1})	5.780	9.901	K_F ($(mgg^{-1})(Lmg^{-1})^{1/n}$)	0.49	1.26	B_D (mol^2J^{-2})	5.9×10^{-6}	1.5×10^{-6}
R^2	0.959	0.976	R^2	0.920	0.948	R^2	0.914	0.896

Table 5. Langmuir adsorption equilibrium parameter at different initial Cr(VI) concentrations

C_o (mgL^{-1})	R_L	
	SSP	CFP
10	0.645	0.508
20	0.476	0.340
30	0.377	0.256
40	0.313	0.205
50	0.267	0.171
60	0.233	0.147
70	0.206	0.128

between the aqueous and solid phases, resulting in higher probability of collision between Cr(VI) ions and sorbents. This also results in higher metal uptake [72].

The adsorption isotherms were studied by varying the initial concentration of chromium ion. Langmuir, Freundlich and D-R models were evaluated for description of metal sorption isotherms (Table 4). Both Langmuir and Freundlich adsorption isotherm models were found to be applicable to this adsorption system, in terms of relatively high regression values compared to that of D-R model. A similar observation of fitting well the adsorption data with the Langmuir and Freundlich isotherm models was observed in adsorption studies on the removal of hexavalent chromium from aqueous solution using a low cost fertilizer industry waste material [18], husk of Bengal gram (*Cicer arientinum* [16], whereas, Langmuir isotherm model fitted the results quite well, suggesting that (a) the surface of the sorbent is homogeneous, (b) all sites are energetically equivalent and each binding site accepts only one Cr(VI) molecule, (c) the sorbed molecules are organized as a monolayer and (d) no interaction occurs between sorbed molecules in the Cr(VI) removal by waste pomace of olive oil factory [46] and chitosan [65].

The essential characteristics of the Langmuir isotherms can be expressed in terms of a dimensionless constant separation factor or equilibrium parameter, R_L, which is defined as $1/(1+K_LC_o)$, where K_L is the Langmuir constant and C_o is the initial concentration of Cr(VI). The R_L value indicates the shape of isotherm as given in Table 5. The separation factor (R_L) values give information about characteristics of adsorption isotherms (Langmuir). Unfavorable, linear, favorable and irreversible adsorptions can be expected when $R_L>1$, $R_L=1$. $0<R_L<1$ and $R_L=0$, respectively [77].

Dubinin-Radushkevich (D-R) isotherm (Table 1) is an empirical model which is generally applied to express the adsorption mechanism with a Gaussian energy distribution onto a heterogeneous surface [41]. Sorption energy (B_D) is a constant related to the mean free energy of adsorption per mole of the adsorbate as it is transferred to the surface of the solid from infinite distance in solution. Sorption energy value for CFP is lower compared to that of SSP (Table 4), which is in parallel to their enthalpy values (Table 2). Hence, higher amount of metal is removed by CFP compared to SSP under similar conditions.

Table 6. Comparison of adsorption capacities of CFP and SSP with different sorbents for Cr(VI) removal

Adsorbent	Maximum adsorption capacity (mgg^{-1})	Reference
Cactus leaves	7.08	[14]
Almond	10.62	[14]
Carbon slurry	15.24	[18]
Maize corn cob	0.28	[42]
Jatropha oil cake	0.82	[42]
Sugarcane bagasse	0.63	[42]
Rice straw	3.15	[78]
Bagasse fly ash	4.35	[79]
Sorghum stem powder	5.78	This study
Casuarinas fruit powder	9.90	This study

A comparison of the chromium ions uptake capacities of CFP and SSP with other biomaterial based sorbents is presented in Table 6. A direct comparison is not possible because the differences in metal uptake capacities are due to a variety of parameters and conditions employed in each referenced work.

CONCLUSION

Biosorption observations on the ability of two agricultural waste materials, CFP and SSP to remove Cr(VI) indicate them as the biomass having potential application to sequester heavy metals from low concentration waste waters. Crude fiber composed of cellulose, hemicelluloses, lignin etc. in SSP, and α-pinene, benzaldehyde, 1,8 cineole, furanoid, α-campholenal, 4-terpineol, α-terpineol etc. in CFP indicates the presence of functional groups like acid, alcohol and amine, which facilitates them as capable adsorbents for participation in ion exchange. As these CFP and SSP are agro-wastes, they have negligible cost and have also proved to be an efficient biosorbent for the removal of Cr(VI) ions.

ACKNOWLEDGEMENTS

The authors are highly thankful to Acharya Nagarjuna University for providing the support for conducting the research work. Authors are also wish to thank SAIF, IIT, Madras for providing

SEM-EDX instrumentation facility and Chemistry Research Centre, Bangalore Institute of Technology, Bengaluru for providing BET surface area and pore distribution analysis facility.

REFERENCES

1. R. S. Juang and R. C. Shiau, *J. Membr. Sci.*, **165**, 159 (2000).
2. J. C. Igwe and A. A. Abia, *The Physical Scientist*, **2**, 83 (2003).
3. P. Rana, N. Mohan and C. Rajagopal, *Water Res.*, **38**, 2811 (2004).
4. World Health Organization (WHO), Guidelines for Drinking-water Quality, 3rd Ed., Recommendations, Geneva (2004).
5. S. Park and W. Y. Jung, *Carbon Sci.*, **2**, 15 (2001).
6. US Department of Health and Human Services, Toxicological Profile for Chromium, Public Health Service Agency for Toxic substances and Diseases Registry, Washington, DC (1991).
7. M. Cieslak-Golonka, *Polyhedron*, **15**, 3667 (1996).
8. P. T. Orr, G. L. Jones and G. R. Hamilton, *Water Res.*, **38**, 4455 (2004).
9. N. K. Hamadi, X. D. Chen, M. M. Farid and M. G. Q. Lu, *J. Chem. Eng.*, **84**, 95 (2001).
10. K. Selvi, S. Pattabhi and K. Kadirvelu, *Bioresour. Technol.*, **80**, 87 (2001).
11. D. D. Das, R. Mahapatra, J. Pradhan, S. N. Das and R. S. Thakur, *J. Colloid Interface Sci.*, **232**, 235 (2000).
12. K. S. Low, C. K. Lee and C. Y. Lee, *Appl. Biochem. Biotechnol.*, **90**, 75 (2001).
13. E. Demirbasa, M. Kobyab, E. Senturkb and T. Ozkana, *Water SA*, **30**, 533 (2004).
14. M. Dakiky, M. Khamis, A. Manassara and M. Mereb, *Adv. Environ. Res.*, **6**, 533 (2002).
15. M. Kobya, *Adsorp. Sci. Technol.*, **22**, 51 (2004).
16. N. Ahalya, R. D. Kanamadi and T. V. Ramachandra, *Electron. J. Biotechnol.*, **8**, 258 (2005).
17. V. K. Gupta, A. K. Shrivastava and J. Neeraj, *Water Res.*, **35**, 4079 (2001).
18. V. K. Gupta, A. Rastogi and A. Nayak, *J. Colloid Interface Sci.*, **342**, 135 (2010).
19. Q. Liu, B. Yang, L. Zhang and R. Huang, *Korean J. Chem. Eng.*, **32**, 1314 (2015).
20. Y. Fan, R. Yang, Z. Lei, N. Liu, J. Lv, S. Zhai, B. Zhai and L. Wang, *Korean J. Chem. Eng.*, **32**, 1 (2015).
21. M. H. Dehghani, D. Sanaei, I. Ali and A. Bhatnagar, *J. Mol. Liq.*, **215**, 671 (2016).
22. H. W. Kwak, M. K. Kim, J. Y. Lee, H. Yun, M. H. Kim, Y. H. Park and K. H. Lee, *Algal Res.*, **7**, 92 (2015).
23. J. B. Dima, C. Sequeiros and N. E. Zaritzky, *Chemosphere*, **141**, 100 (2015).
24. E. Fourest and J. C. Roux, *Appl. Microbiol. Biotechnol.*, **37**, 399 (1992).
25. P. M. Ramya, N. R. Venkata, M. Jayasravanthi and B. J. Dulla, *Global Nest J.*, **17**, 291 (2015).
26. B. Ramavandi, G. Asgari, J. Faradmal, S. Sahebi and B. Roshani, *Korean J. Chem. Eng.*, **31**, 2207 (2014).
27. G. V. V. Aditya, B. P. Pujitha, N. C. Babu and P. Venkateswarlu, *Korean J. Chem. Eng.*, **29**, 64 (2012).
28. R. Jayakumar, M. Rajasimman and C. Karthikeyan, *Korean J. Chem. Eng.*, **32**, 2031 (2015).
29. A. B. Wassie and V. C. Srivastava, *J. Environ. Chem. Eng.*, **4**, 1117 (2016).
30. S. Rangabhashiyam and N. Selvaraju, *J. Taiwan Inst. Chem. E.*, **47**, 59 (2015).
31. S. Arris, M. B. Lehocine and A. H. Meniai, *Int. J. Hydrogen Energy*, **1**, 1 (2014).
32. R. Jayakumar, M. Rajasimman and C. Karthikeyan, *J. Environ. Chem. Eng.*, **2**, 1261 (2014).
33. S. Kuppusamy, P. Thavamani, M. Megharaj, K. Venkateswarlu, Y. B. Lee and R. Naidu, *Process Saf. Environ.*, **100**, 173 (2016).
34. F. V. Hackbarth, D. Maass, A. A. U. de Souza, V. J. Vilar and S. M. G. U. de Souza, *Chem. Eng. J.*, **290**, 477 (2016).
35. M. O. Omorogie, J. O. Babalola, E. I. Unuabonah, W. Song and J. R. Gong, *J. Saudi Chem. Soc.*, **20**, 49 (2012).
36. R. O. Ogbodu, M. O. Omorogie, E. I. Unuabonah and J. O. Babalola, *Environ. Prog. Sustain. Energy*, **34**, 1694 (2015).
37. M. O. Omorogie, J. O. Babalola, E. I. Unuabonah and J. R. Gong, *Environ. Technol.*, **35**, 611 (2014).
38. N. A. Reddy, R. Lakshmipathy and N. C. Sarada, *Alexandria Eng. J.*, **53**, 969 (2014).
39. J. Kanagaraj, T. Senthilvelan, R. C. Panda, R. Aravindhan and A. B. Mandal, *Chem. Eng. Technol.*, **37**, 1741 (2014).
40. J. R. Deans and B. G. Dixon, *Water Res.*, **26**, 469 (1992).
41. K. Y. Foo and B. H. Hameed, *Chem. Eng. J.*, **156**, 2 (2010).
42. J. P. Chen and L.Yang, *Ind. Eng. Chem. Res.*, **44**, 9931 (2005).
43. Annual book of ASTM standards part - 23, American Society for Testing and Materials, Philadelphia (1972).
44. S. Lagergren, *Handlingar*, **24**, 1 (1898).
45. Y. S. Ho and G. McKay, *Process Biochem.*, **34**, 451 (1999).
46. E. Malkoc, Y. Nuhoglu and M. Dundar, *J. Hazard. Mater.*, **B138**, 142 (2006).
47. F. Rafia and A. H. Gilani, *Asian-Australasian Journal of Animal Sciences*, **14**, 935 (2001).
48. I. A. Ogunwande, G. Flamini, A. E. Adefuye, N. O. Lawal, S. Moradeyo and N. O. Avoseh, *S. Afr. J. Bot.*, **77**, 645 (2011).
49. J. Lerivrey, B. Dubois, P. Decock, J. Micera and H. Kozlowski, *Inorg. Chim. Acta*, **125**, 187 (1986).
50. A. K. Bhattacharya, S. N. Mandal and S. K. Das, *Chem. Eng. J.*, **123**, 43 (2006).
51. P. Homagai, H. Paudyal and G. Kedarnath, *J. Nepal Chem. Soc.*, **23**, 102 (2009).
52. K. K. Panday, G. Prasad and V. N. Singh, *J. Chem. Techol. Biotechnol. A - Chemical Technology*, **34**, 367 (1984).
53. F. N. Acar and E. Malkoc, *Bioresour. Technol.*, **94**, 13 (2004).
54. G. S. Agarwal, H. K. Bhuptawat and S. Chaudhari, *Bioresour. Technol.*, **97**, 949 (2006).
55. D. C. Sharma and C. F. Forster, *Water Res.*, **27**, 1201 (1993).
56. D. C. Sharma and C. F. Forster, *Bioresour. Technol.*, **49**, 31 (1994).
57. D. C. Sharma and C. F. Forster, *Water SA*, **22**, 153 (1996).
58. S. S. Ahluwalia and G. Dinesh, *Bioresour. Technol.*, **98**, 2243 (2007).
59. J. C. Igwe, D. N. Ogunewe and A. A. Abia, *Afr. J. Biotechnol.*, **4**, 1113 (2005).
60. K. R. Reddy, T. Xie and S. Dastgheibi, *J. Environ. Sci. Health*, **49**, 524 (2014).
61. U. K. Garg, M. P. Kaur, V. K. Garg and D. Suda, *J. Hazard. Mater.*,

140, 60 (2007).
62. P. R. Puranik and K. M. Paknikar, *Biotechnology Progress*, **15**, 228 (1999).
63. C. Selomulya, V. Meeyoo and R. Amal, *J. Chem. Technol. Biotechnol.*, **74**, 111 (1999).
64. G. Cimino, A. Passerini and G. Toscano, *Water Res.*, **34**, 2955 (2000).
65. R. Schmuhl, H. M. Krieg and K. Keizer, *Water SA*, **27**, 1 (2001).
66. B. R. Reddy, N. Mirghaffari and I. Gaballah, *Resour. Conserv. Recycl.*, **21**, 227 (1997).
67. P. Srinivas Rao, R. Shashikant and G. S. Munjunatha, *J. Environ. Sci. Health A*, **27**, 2227 (1992).
68. J. H. An and S. Dultz, *Clays Clay Miner.*, **56**, 549 (2008).
69. N. Bishnoi, M. Bajaj, N. Sharma and A. Gupta, *Bioresour. Technol.*, **91**, 305 (2004).
70. D. Park, S. Y. Yun and J. M. Park, *Chemosphere*, **60**, 1356 (2005).
71. D. Park, Y. S. Yun and J. M. Park, *Environ. Sci. Technol.*, **38**, 4860 (2004).
72. N. Tewari, P. Vasudevan and B. K. Guha, *Biochem. Eng. J.*, **23**, 185 (2005).
73. J. Dai and R. J. Mumper, *Molecules*, **15**, 7313 (2010).
74. B. R. Sudha and E. Abraham, *Bioresour. Technol.*, **87**, 17 (2003).
75. S. Niyogi, E. T. Abraham and S. V. Ramakrishna, *J. Sci. Ind. Res. India*, **57**, 809 (1998).
76. S. Larous, A. H. Meniai and M. B. Lehocine, *Desalination*, **185**, 483 (2005).
77. G. Mckay, H. S. Blair and J. R. Gardener, *J. Appl. Polym. Sci.*, **27**, 3043 (1982).
78. H. Gao, Y. Liu, G. Zeng, W. Xu, T. Li and W. Xia, *J. Hazard. Mater.*, **150**, 446 (2008).
79. V. K. Gupta and I. Ali, *J. Colloid Interface Sci.*, **271**, 321 (2004).